THE JOURNAL OF BIOLOGICAL CHEMISTRY Vol. 277, No. 3, Issue of January 18, pp. 2287–2301, 2002
Printed in U.S.A.

Reduced Cell Surface Expression of CCR5 in CCR5Δ32 Heterozygotes Is Mediated by Gene Dosage, Rather Than by Receptor Sequestration*

Received for publication, August 29, 2001, and in revised form, October 9, 2001
Published, JBC Papers in Press, October 16, 2001, DOI 10.1074/jbc.M108321200

Sundararajan Venkatesan‡§, Ana Petrovic‡, Donald I. Van Ryk‡, Massimo Locati¶, Drew Weissman‖, and Philip M. Murphy**

*From the ‡Laboratory of Molecular Microbiology and **Laboratory of Host Defenses, NIAID, National Institutes of Health, Bethesda, Maryland 20892, ¶Istituto di Patologia Generale, Via Mangiagalli, Milano, 20133 Italy, and the ‖Division of Infectious Diseases, University of Pennsylvania, Philadelphia, Pennsylvania 19104*

Macrophage tropic (M-tropic) human immunodeficiency virus (HIV) infection of primary human T cells and macrophages requires optimal cell surface expression of the chemokine receptor CCR5 in addition to CD4. Natural mutations of CCR5 that impair surface expression bestow in the homozygous state complete resistance to M-tropic HIV infection. *ccr5Δ32* is the major prototype of such mutants. *ccr5Δ32* heterozygosity is associated with delayed onset of AIDS and reduced risk of initial transmission, and this correlates with reduced levels of CCR5 and reduced infectability of CD4+ cells. In addition to gene dosage, sequestration of wild type (WT) CCR5 by mutant protein has been proposed as a mechanism to explain reduced surface expression of CCR5 in cells from *ccr5Δ32* and *CCR5-893*(−) heterozygotes. However, here we demonstrate that a molar excess of *ccr5Δ32* or related deletion mutants does not significantly impair the cell surface density of co-expressed WT receptor either in human epithelial cells or Jurkat T cells. Further, ligand-dependent signaling and M-tropic HIV usage of WT receptor are also unaffected. Nascent WT receptor does associate with *ccr5Δ32* and related mutant proteins and with other unrelated CC and CXC chemokine receptors under transient labeling conditions. However, using confocal microscopy, we demonstrate that in the steady state, WT and truncated CCR5 proteins segregate into nonoverlapping subcellular compartments. These findings together with the observed and known variability in the cell surface density of CCR5 on quiescent PBLs lead us to conclude that reduced CCR5 gene dosage rather than receptor sequestration is the major determinant of reduced CCR5 expression in cells from *ccr5Δ32* heterozygotes.

Chemokine receptors as members of the superfamily of GPCRs[1] share a common three-dimensional structure composed of heptahelical transmembrane (TM) domains, which define multiple extracellular and intracellular loops (1–3). Some members of the human chemokine receptor family serve as co-receptors for HIV entry (4–7) besides their essential roles in regulating leukocyte chemotaxis in inflammation (8, 9). M-tropic and T-tropic viruses use preferentially CCR5 and CXCR4, respectively. Based on this dichotomy, M-tropic and T-tropic viruses may be referred to as R5 and X4 strains (4–6, 10). Consistent with this designation, virus replication of R5 strains is inhibited *in vitro* by cognate CCR5 ligands such as MIP-1α, MIP-1β, and RANTES (11, 12). By the same criteria, the CXCR4 ligand SDF-1 inhibits X4 strain replication (13, 14).

Relative cell surface levels of CD4 and chemokine receptors modulate primary HIV infection. Naturally occurring mutations in the co-receptors and their cognate ligands influence HIV transmission and AIDS progression. Among CCR5 mutants, a naturally occurring 32-bp deletion, commonly observed in Caucasoid subjects and referred to as *ccr5Δ32*, affords complete immunity in the homozygous state to M-tropic HIV infection of PBMCs (15–17). *ccr5Δ32* has a frameshift at the 185th residue in the second ECL of CCR5 that tethers 33 residues in the +2 frame at this site. Another natural variant of CCR5, *CCR5-893*(−) observed exclusively in Asians, terminates prematurely at the 299th residue, resulting from a frameshift that fuses 10 residues of the −1 frame and therefore lacks the natural C-tail (18, 19). Both proteins derived from *ccr5Δ32* and *CCR5-893*(−) are retained in the ER and not expressed at the cell surface (19, 20). Epidemiological studies have linked the *CCR5*/*ccr5Δ32* heterozygotic state to a delay in the onset of AIDS (15, 17, 22), and more recently, *CCR5*/*ccr5Δ32* heterozygotes were shown to possess a higher degree of resistance against HIV infection than the WT (*CCR5*/*CCR5*) counterparts (23). FACS analysis of cell surface CCR5 density in fresh PBMCs of a large number of donors showed that, despite considerable individual variability, *CCR5*/*ccr5Δ32* heterozygotes had significantly lower levels of CCR5 than WT homozygotes. Further, a direct correlation between steady state levels of CCR5 and M-tropic HIV infectability was established (17, 24).

Two reports have addressed mechanisms underlying CCR5 deficiency at the cell surface in *ccr5Δ32* and *CCR5-893*(−) heterozygotes. Histological analysis of HeLa cells co-transfected with *ccr5Δ32* and WT receptor demonstrated trapping of the WT receptor by the mutant in the ER and loss of cell surface

* The costs of publication of this article were defrayed in part by the payment of page charges. This article must therefore be hereby marked "*advertisement*" in accordance with 18 U.S.C. Section 1734 solely to indicate this fact.

§ To whom correspondence should be addressed: LMM, NIAID, Bldg. 10, Rm. 6A05, National Institutes of Health, Bethesda, MD 20892-1576. Tel.: 301-496-6359; Fax: 301-402-4122; E-mail: aradhana@helix.nih.gov.

[1] The abbreviations used are: GPCR, G protein-coupled receptor; AMLV, amphotropic murine leukemia virus; APC, allophycocyanin; CKR, chemokine receptor; ECL, extracellular loop; ER, endoplasmic reticulum; FITC, fluorescein 5-isothiocyanate-conjugated; HIV, human immunodeficiency virus; *luc*, luciferase; mAb, monoclonal antibody; MFV, mean fluorescence value; MIP, macrophage inflammatory protein; M-tropic, macrophage tropic; PBS, phosphate-buffered saline; PE, phycoerythrin; RANTES, regulated on activation normal T cell expressed and secreted; SDF, stromal cell derived factor; TC, tricolor; TM, transmembrane; T-tropic, T-cell tropic; WT, wild type; FACS, fluorescence-activated cell sorting; PBMC, peripheral blood mononuclear cell.

expression of WT receptor (20). Simultaneous infection of Jurkat T cells with recombinant Sendai viruses encoding WT CCR5 and the *CCR5-893*(−) mutant was shown to decrease the cell surface density of WT receptor by FACS analysis (19). Overexpression of *ccr5Δ32* and related deletion mutants was shown to inhibit M-tropic HIV usage of co-transfected WT receptor in HeLa-CD4 cells encoding an indicator gene. Further, using a yeast two-hybrid system, it was shown that CCR5 was capable of dimerizing with itself or C-terminally truncated deletion mutants (20). These findings were interpreted to suggest that *ccr5Δ32* and *CCR5-893*(−) mutant proteins dominantly interfered with the functional expression of wt CCR5 by heterodimerization with and cytoplasmic sequestration of WT protein.

In this study, we have examined the effect of *ccr5Δ32* and related deletion mutants on the expression and function of WT CCR5 in a system that controlled for gene expression. In contrast to the previous reports, we found that overexpression of CCR5 deletion mutants did not significantly affect the surface presentation or function of WT receptor. WT CCR5 protein did physically associate with the various deletion mutants under nascent labeling conditions, but such transient associations also occurred between CCR5 and other CC and CXC chemokine receptors and did not appear to be functionally relevant. The implications of these findings and possible reasons for the discrepancy with the earlier reports are discussed.

MATERIALS AND METHODS

Expression Plasmids—Construction of the Rous sarcoma virus long terminal repeat- or cytomegalovirus immediate early promoter-linked expression plasmids for WT CCR2B, CCR3, CCR5, CXCR1, and CXCR2 has been described (4, 25–28). The various mutants described in this paper were constructed *in vitro* by the overlap PCR method (29) and cloned using a commercial vector, pCDNA3.1 directional TOPO vector (Invitrogen Corp., Rockville, MD). Some of the mutants were also cloned into FLAG vector (Sigma) that appended a FLAG epitope at the N terminus of the indicated mutants. Δ32 CCR5 open reading frame was PCR-amplified from the T cell DNA of a CCR5Δ32 homozygotic individual and cloned into pCR3.1 vector.

DNA Transfection—Monolayers were transfected by the $CaCl_2$ method (Promega Corp., Madison, WI) or by lipofection using Fugene (Roche Molecular Biochemicals). The JJK line of Jurkat T cells (contributed by Dan Littman; Columbia University, New York) in RPMI medium containing 10% fetal calf serum was transfected by use of a Bio-Rad electroporator at a setting of 250 V and 960 microfarads.

HIV Infectivity Measurement—Pseudotyped HIV stocks expressing firefly luciferase (*luc*) in place of Nef were prepared by transfecting 293-T cells (by $CaCl_2$ precipitation) with 5 μg each of defective HIV provirus, pNL4–3 Env(−) vpR(−) *luc*(+), and plasmids encoding *env* genes from AMLV and M-tropic HIV strains, JRFL (obtained through the NIH AIDS Research and Reference Reagent Program, Rockville, MD), AD88, and T-tropic HIV NL4–3. Virus in the culture supernatants was quantified by reverse transcriptase assay and adjusted to constant reverse transcription units/ml.

293-T cells were transfected with an equimolar mixture of WT CCR5 and CD4 lacking the C-tail (truncated CD4, known as tCD4) and, where indicated, with a 2.5-fold molar excess (over WT CCR5) of Δ4, Δ8, and Δ32 mutant CCR5 plasmids. After checking the transfection efficiency by FACS analysis, CD4+ cells were purified by binding to and elution from CD4 antibody-coated magnetic beads using a commercial kit (Dynal Inc., Lake Success, NY) that resulted in recovery of >90% CD4+ cells. Eluted cells were seeded into 48-well plates ($0.5–1 \times 10^5$ cells/well) and infected in triplicate with the respective pseudotyped *luc*-expressing HIVs. Virus particles without *env* served as negative control, while AMLV *env* pseudotyped virus served as an HIV-irrelevant control. An identical number of untransfected cells were infected by the same viruses. For comparing the relative efficiencies of HIV entry, *luc* expression induced by AMLV pseudotyped virus was adjusted to constant levels. For this purpose, AMLV pseudotyped virus infection was performed on transfectants prior to CD4 immune selection. At 24–30 h after infection, cell lysates were assayed for luciferase activity using a commercial kit (Promega Corp.) and a microplate luminometer (Multex, Dynex Technologies, Chantilly, VA).

Immunological Reagents and Methods—The following monoclonal antibodies (mAbs) or rabbit antisera were used to identify CCR5 and other chemokine receptors: 1) for CCR5, FITC- or APC-conjugated mAb 2D7, PE-conjugated mAb 3A9 (BD-Pharmingen, San Diego, CA), FITC-conjugated mAb 181 and 182 (R & D Systems), unconjugated mAbs 2D7, 3A9, 180, and 182 (National Institutes of Health AIDS Research and Reference Reagent Program, Rockville, MD), and rabbit antibody against the N-terminal end of CCR5 (27); 2) for CCR2, mAb, clone 48607 (R & D Systems); 3) for CCR3, mouse mAb clone, 7B1 (National Institutes of Health AIDS Research and Reference Reagent Program); 4) for CXCR1, mAb CDw128 (BD-Pharmingen, San Diego, CA); 5) for CXCR2, mAb, clone 48311 (R & D Systems) or unconjugated mAb, IL-8-Rb (BD-Pharmingen). For detecting CD4, FITC- or PE-conjugated mAb Leu 3A (BD-Pharmingen) or APC- or tricolor (TC)-conjugated mAb S3.5 (Caltag Laboratories, Burlingame, CA) was used. For CD8 detection, FITC- or PE-conjugated mAb Leu 2A (BD-Pharmingen), or mAb 3B5 conjugated with APC or TC (Caltag Laboratories, Burlingame, CA) was used. For secondary staining, dye-conjugated purified Fab fragments with the relevant species-specific reactivity were obtained from commercial sources (Molecular Probes, Inc., Eugene, OR; Jackson Immunoresearch Laboratories, West Grove, PA). Antibody binding and flow cytometric analysis protocols have been described before (30).

Metabolic Labeling and Immunoprecipitation—For metabolic labeling experiments, 293-T cells (10^6 to 10^7) at 24–30 h after transfection (as described in the appropriate figure legends) were rinsed three times with and incubated in methionine- and cysteine-free Dulbecco's modified Eagle's medium containing 1% dialyzed fetal calf serum (0.2 ml/sample) for 10 min. Cells were labeled for 30 min by the addition of [^{35}S]Trans-label (ICN Biomedicals Inc. Costa Mesa, CA) to 1 mCi/ml. For measuring the kinetics of protein biosynthesis, 2×10^7 cells were labeled for 15 min in 500 μl of labeling medium (1 mCi/ml), followed by a metabolic chase in 20 volumes of complete growth medium. Conditions for processing labeled cells, SDS-PAGE and PhosphorImager analysis (Molecular Dynamics, Inc., Sunnyvale, CA; Amersham Biosciences, Inc.) have been described (30).

For measuring ligand-dependent CCR5 phosphorylation, 293-T cells (two T25 flask equivalents) were co-transfected with WT CCR5 and CD8 alone or with different amounts of CCR5 deletion mutants as indicated in the figure legend. Cells were harvested by incubation at 37 °C for 10 min with PBS containing 5 mM EDTA, an aliquot of each sample was tested for CD8 expression by FACS analysis, and the remaining cells were rinsed three times and incubated as a suspension culture in complete growth medium at 37 °C. Individual transfectants were adjusted to reflect a similar percentage of CD8+ cells and rinsed with 20 volumes of 2× HEPES-buffered, phosphate-deficient RPMI and incubated (4×10^6 cells/ml) in the same medium containing 1.5% dialyzed fetal bovine serum for 30 min at 37 °C. HEK-293 (2×10^6) cells stably expressing WT CCR5 provided the positive control for the assay. The cells were then incubated for 30 min with [^{32}P]orthophosphate (0.5 mCi/ml) in the presence of okadaic acid (1 μM). Cells were stimulated with 100 nM MIP-1β or RANTES (purchased from Peprotech Inc., Rocky Hill, NJ) for 15 min followed by processing for immunoprecipitation, SDS-PAGE, and PhosphorImager analysis as described (30).

For co-precipitation experiments, 293-T cells were co-transfected with WT CCR5, tagged at the C terminus with six histidines (WT-His_6) and the indicated CCR mutants carrying a FLAG epitope at the respective N termini. Other transfections included pairwise combinations of WT-His_6 with the Δ32 mutant or expression plasmids for CCR2B, CXCR1, or CXCR2. Transfections were labeled for 30 min with [^{35}S]methionine (Amersham Biosciences) to 0.5 mCi/ml, and cell extracts were prepared as described. After preclearing the cell extracts with protein G-agarose, the samples were divided in half and immunoprecipitated with FLAG-specific (Sigma) or His_6-specific mAb (CLONTECH; BD-Pharmingen) prebound to protein G beads. CCR5Δ32 protein was precipitated with rabbit IgG against Δ32 frameshift sequence, and the other chemokine receptors were precipitated with the respective mAbs described above.

Confocal Immunofluorescence Microscopy—For immunofluorescence detection of receptors on live cells, transfected cells plated on coverslips were rinsed with PBS and reacted with receptor-specific antibodies in PBS containing 0.3% bovine serum albumin for 30 min at 4 °C. For WT CCR5 and certain deletions, FITC- or APC-conjugated 2D7 (BD-Pharmingen) or FITC-conjugated 182 (R & D Systems) mAbs were used. Since these and some other mAbs failed to recognize deletions extending upstream of the third intracellular loop (Δ8 equivalent), transfections were also checked with rabbit serum against the 26-residue MDYQVSSPIYDINYYTSEPCQKINVK N-terminal sequence of CCR5. For specific detection of CCR5Δ32 protein, we generated rabbit anti-

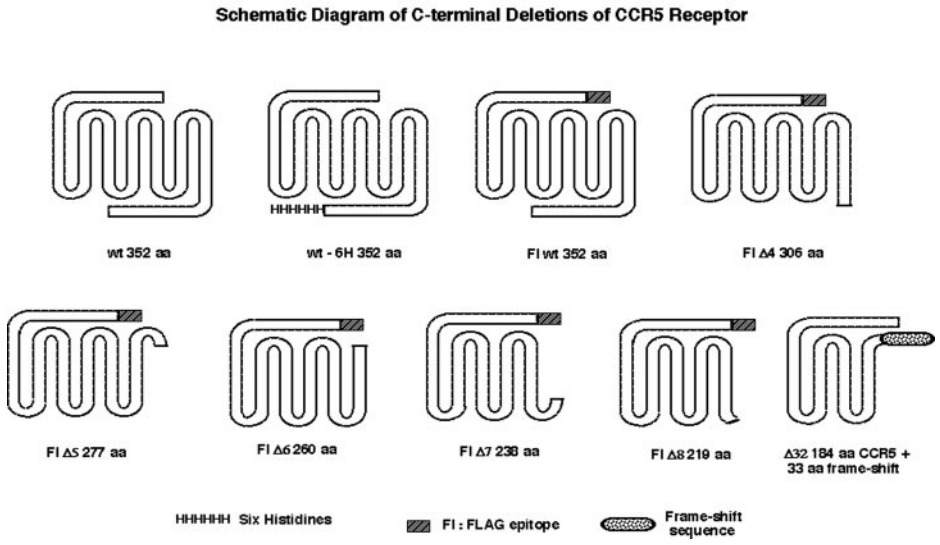

FIG. 1. **Schematic diagram of CCR5 mutants.** C-terminal deletions of CCR5 that progressively excise the C-terminal tail and distal TM domains and the various ECLs and intracellular loops are depicted pictorially. Some of the constructs were tagged with FLAG (Fl) epitope at the N terminus or six histidines (6H) at the C terminus. The FLAG-tagged CCR5 truncation mutants shown here and labeled Δ4–Δ8 represent additional members of the previously described (30) family of C-terminally truncated CCR5 mutants. The naturally occurring CCR5Δ32 mutant that results in a frameshift fusion of 33 amino acids (*aa*) to the CCR5 sequence at the 184th position in the second ECL represents the longest C-terminal deletion.

serum against a keyhole limpet hemocyanin-conjugated 12-residue CHGHLLLGNPKNSASVSK C-terminal peptide corresponding to the frameshift sequence in the CCR5Δ32 gene. Rabbit antisera against CCR5 peptides were titrated to determine the optimal dilution that gave the best signal/noise ratio in immunofluorescence assays when used in combination with 1:500 dilutions of Alexa 568 or FITC second antibodies. FLAG epitope was detected using FITC FLAG mAb or by use of M2 murine mAb and rabbit IgG against FLAG peptide as first antibodies (Sigma) followed by chromophore-tagged second antibodies. In cases where first antibodies were unlabeled, the coverslips were rinsed five times with PBS and stained with second antibodies (Fab) fragments, conjugated with APC, FITC, Texas Red, or Alexa dyes 488, 568, or 630 obtained commercially (Molecular Probes; Jackson Immunoresearch Laboratories) in PBS containing 0.3% bovine serum albumin for 30 min at 4 °C. After rinsing five times with PBS, the coverslips were mounted in Fluoromount-G (Southern Biotechnologies, Birmingham, AL). For detecting intracellular antigens, cells were fixed in 4% (v/v) paraformaldehyde for 15 min at 4 °C, rinsed five times with PBS, permeabilized by a 15-min treatment with 0.25% Triton X-100 (or Nonidet P-40) in PBS at 25 °C, and reacted as above with the respective antibody combinations. The following organelle-specific antibodies were used to detect co-localization of the receptors with various subcellular compartments: 1) for ER, mAbs (Affinity Bioreagents, Golden, CO) or rabbit sera against calnexin or calreticulin (Stressgen Biotechnologies Corp., Victoria, Canada); 2) for Golgi, Deng mAb, and 3) for plasma membrane, anti-transferrin receptor (CD71, from Beckman-Coulter) or mAb against Na^+/K^+ ATPase (Affinity Bioreagents, Golden, CO). Images were collected on a Leica TCS-NT/SP confocal microscope (Leica Microsystems, Exton, PA) and analyzed as described (30).

Intracellular [Ca^{2+}] Measurements—293-T cells were co-transfected with CD4 and WT CCR5 together with 4-fold molar excess of vector DNA or the indicated CCR5 deletion mutants. At 36 h post-transfection, aliquots of ~10^5 cells were checked for transfection efficiency by FACS analysis. The remaining cells were adjusted to reflect a constant fraction of CD4+ cells. Transfectants (~10^7/ml) were used for a RANTES-dependent Ca^{2+} flux assay as described (30). All transfectants were also evaluated for Ca^{2+} flux responses to 200 nM concentrations of SDF1-α and/or ATP.

RESULTS

CCR5 Truncation Mutants Are Retained in the ER and Show No Defects in Turnover—To analyze the effects of truncation mutants on the function of WT CCR5, we engineered serial C-terminal CCR5 deletions for transient expression. We have shown previously that an intact C-terminal tail was required for optimal cell surface expression of CCR5, and transport-impaired mutants were retained mostly in the ER/Golgi compartments but displayed no obvious defects in protein turnover (30). To inquire whether larger deletions might display unusual properties of protein processing and interfere with function of WT CCR5, we engineered additional deletions excising sequence up to the fifth TM domain. These mutants are illustrated in Fig. 1 and are labeled Δ*4* through Δ*8*. They were tagged at the N termini with a FLAG epitope, and for comparison, WT CCR5 was tagged similarly. The naturally occurring CCR5Δ32 mutant that replaced the sequence downstream of the second ECL by a frameshift sequence of 33 residues represented the largest deletion mutant.

Steady-state cell surface expression of the mutants shown in Fig. 1 was examined following transfection of 293-T or HeLa cells. CD8 was co-transfected, and the distribution of CD8 and CCR5 was examined by two-color FACS using two different monoclonal antibodies or rabbit antiserum against the CCR5 N terminus. A representative FACS profile is given in Fig. 2*A*. Two-color dot plot analysis of cells co-transfected with WT CCR5 and CD8 revealed a double positive diagonal population with almost equivalent staining for both receptors. By this analysis, none of the CCR5 truncation mutants used was identified at the cell surface. To examine more directly the subcellular distribution of WT and mutant CCR5, we analyzed living HeLa cells transfected with individual mutants by confocal immunofluorescence microscopy. Some of the more commonly used mAbs such as 2D7 and 182 were not reactive with CCR5Δ32 because it lacked the epitope or with Δ8, probably due to misfolding. To ensure uniform antibody reactivity, we used rabbit IgG against N-terminal CCR5 peptide or mAb 180 targeted against an N-terminal epitope. Twelve fields (10–20 cells/field) were examined for each staining from two separate experiments for each antibody. Live cells expressing WT CCR5 exhibited uniform punctate cell surface fluorescence (Fig. 2*B*). Δ4 (terminated at the 306th residue) and all upstream deletions including the natural CCR5Δ32 variant displayed no surface staining. When the transfectants were fixed and permeabilized prior to antibody staining, all of the CCR5 mutants displayed similar levels of intracellular antibody reactivity (Fig. 2*B*).

To examine the intracellular sites of retention of CCR5 mutants, fixed and permeabilized transfectants were immunostained with a mixture of antibodies against CCR5 and the indicated organelle component(s). As discussed in a previous report (30), cells were treated with cycloheximide (50 μg/ml) and anisomycin (25 μg/ml) for 30 min prior to fixation to facilitate clearing of nascent proteins from the ER. Without this treatment, there was substantial retention of both wt and mutant CCR5 in the ER (not shown). With CCR5 pseudocolored in *green* and the organelles in *red*, co-localized regions appear *yellow* (Fig. 3). Co-localization was adjudged only when five successive 0.25 μ confocal planes of each potential co-localized

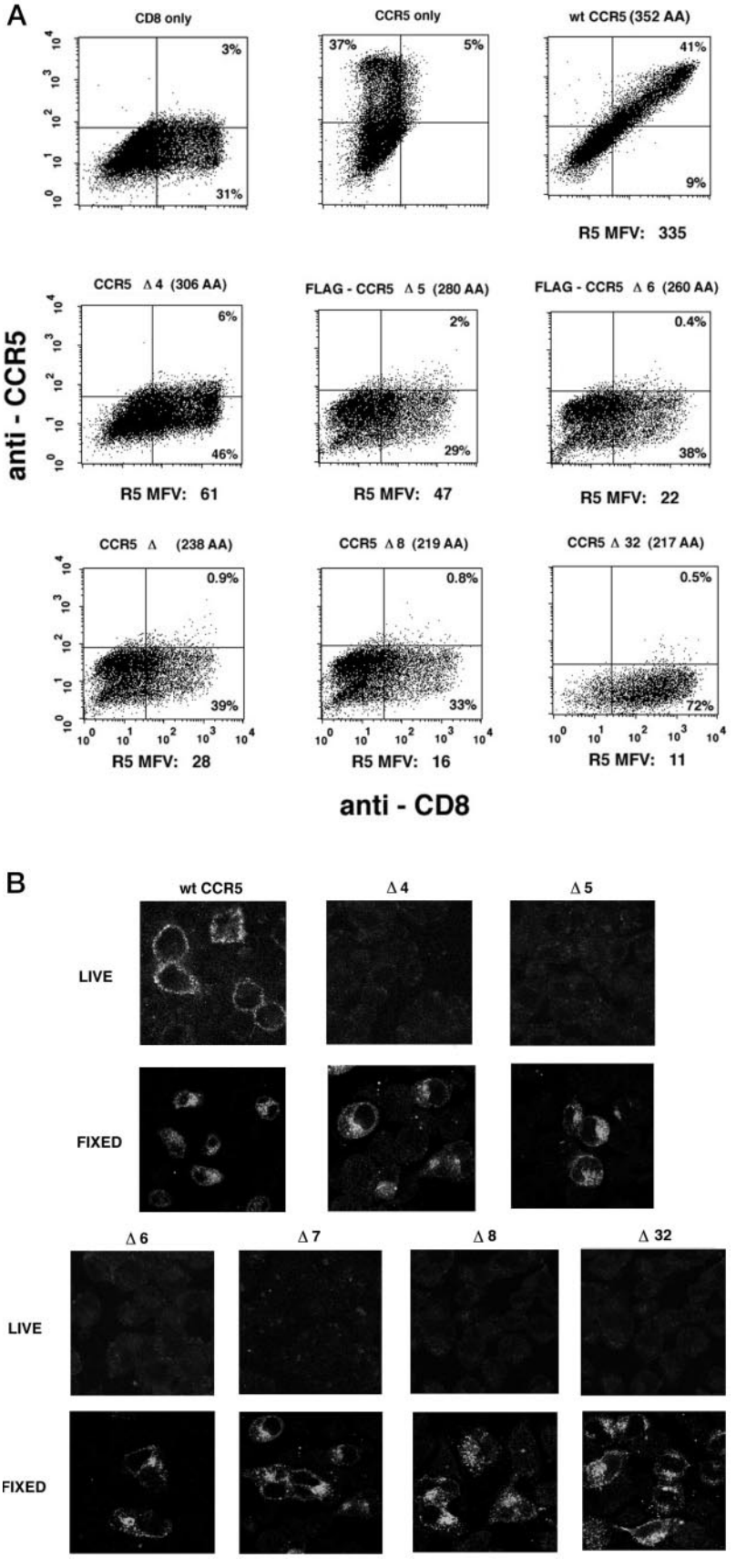

FIG. 2. *A*, cell surface expression of CCR5 truncations evaluated by FACS analysis. Results represent three transfections in 293-T cells. In this experiment, transfectants were stained with a mixture of PE-conjugated CCR5 antibody, 2D7, and APC conjugated CD8 antibody. In all cases, the indicated CCR5 derivative was co-transfected with CD8 except for cells transfected with WT CCR5 or CD8 alone and mock-transfected cells, which set the controls. MFVs of CCR5s were normalized to constant CD8 values. *B*, cellular distribution of CCR5 truncation mutants analyzed by immunofluorescence microscopy. HeLa cells were individually transfected with the indicated CCR5 plasmids. Cell surface CCR5 on living cells was detected by primary reaction of transfectants with rabbit antiserum against CCR5 N-terminal peptide, followed by staining with Texas Red-conjugated goat antibodies (Fab fragments) against rabbit IgG. A parallel set of transfectants were fixed and permeabilized before reaction with the same protocol. Immunofluorescence images were visualized by a 100 × objective of a Leica confocal microscope.

zone displayed similar intensity of co-staining. Under these conditions, WT CCR5 was mostly distributed at or near the periphery of the cells, co-localizing with plasma membrane markers such as Na^+/K^+ ATPase or transferrin receptor (Fig. 3). Neither Δ8 nor CCR5Δ32 was expressed at the cell surface. However, both these mutants displayed a reticular pattern of staining, typical of the ER, and as shown in Fig. 3, they displayed significant co-staining with the ER marker. WT CCR5

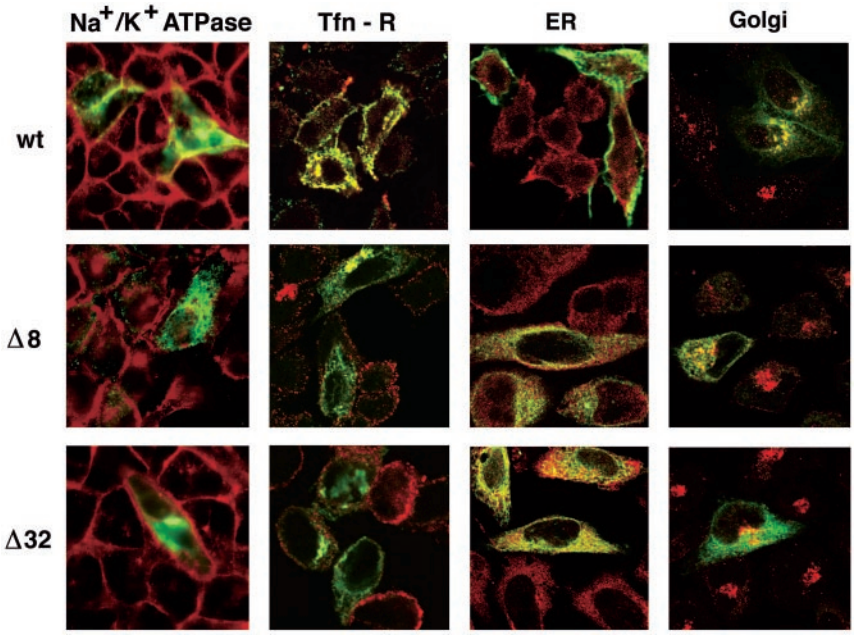

FIG. 3. **Subcellular distributions of WT and mutant CCR5.** HeLa cells transfected with the indicated CCR5 plasmids were treated with cycloheximide for 30 min prior to fixation and detergent treatment. Antibody staining and confocal microscopy are described under "Materials and Methods." For co-staining plasma membrane and CCR5, a mixture of unconjugated CD71 and rabbit IgG against CCR5 N terminus was used. For Golgi visualization, Deng antibody followed by tetramethylrhodamine-5 (and -6)-isothiocyanate-conjugated anti-mouse IgM was used. ER was stained with anti-calreticulin mAb. CCR5 is colored *green*, and the respective organelle markers are in *red*.

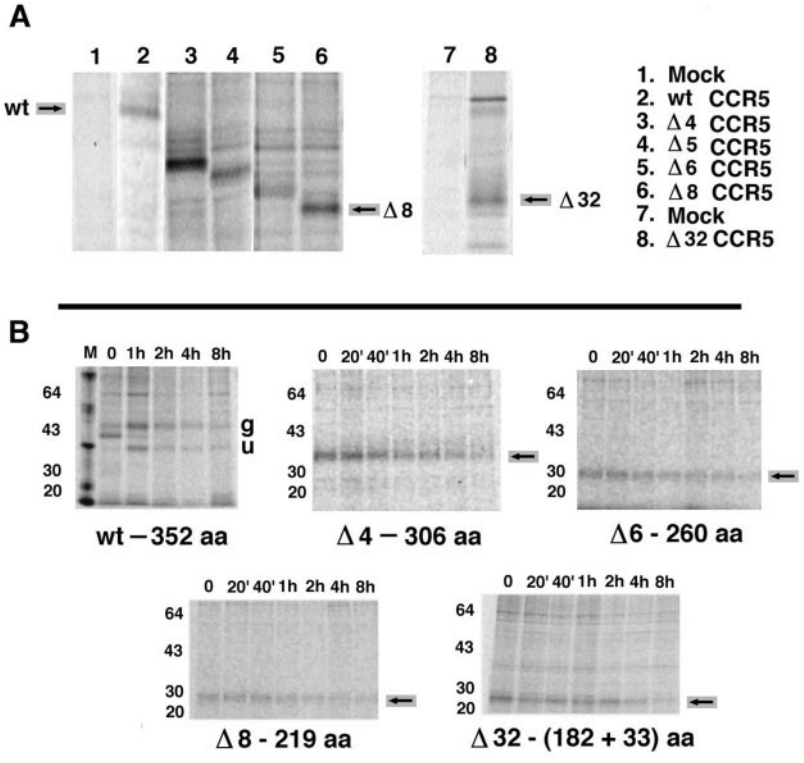

FIG. 4. *A*, immunodetection of *de novo* synthesized WT CCR5 and deletion mutants. An aliquot (10^6 cells) of transfected HEK-293 cells was metabolically labeled and processed for immunoprecipitation of WT and CCR5 mutants. WT CCR5 and all mutants except for CCR5Δ32 were recovered by precipitation using rabbit IgG against CCR5 N-terminal peptide. CCR5Δ32 was precipitated using a rabbit antiserum against the frameshift sequence. A fluorogram of the SDS-PAGE profile is shown. The *arrows* denote WT CCR5, Δ8, and CCR5Δ32 protein bands. *B*, CCR5 deletion mutants do not undergo abnormal metabolic turnover. 293-T cells (2 × 6 well plates for each set) were co-transfected with CD8 and WT CCR5 or the indicated mutants. FACS was used to monitor transfectants for CD8 and CCR5 expression. Cells were labeled for 15 min with [^{35}S]methionine and chased with unlabeled amino acid mix for the indicated times. One-third aliquot from each time point was analyzed for CD8 labeling by SDS-PAGE and PhosphorImager scanning. The remaining aliquots were adjusted to reflect constant CD8 levels for the respective time points, and CCR5 was immunoprecipitated and processed for SDS-PAGE. Scanned images of SDS-PAGE are shown. Chase times are shown *above* each *gel*. *Lane M* refers to molecular mass markers with the respective masses in kDa shown on the *left*. In the *panel* for *WT CCR5*, the letters *g* and *u* identify the *O*-glycosylated and unglycosylated species, respectively. *aa*, amino acids.

showed some co-localization with the Golgi marker. Since protein synthesis was arrested, this fraction of CCR5 localizing in the Golgi probably represented sequestration of recycling receptor in the late Golgi rather than stasis during forward transport. By contrast, neither Δ8 nor CCR5Δ32, which is defective for anterograde transport and therefore incapable of recycling from the cell surface, displayed significant co-localization with the Golgi marker.

We have shown before that transport impaired CCR5 mutants did not display accelerated intracellular turnover (30).

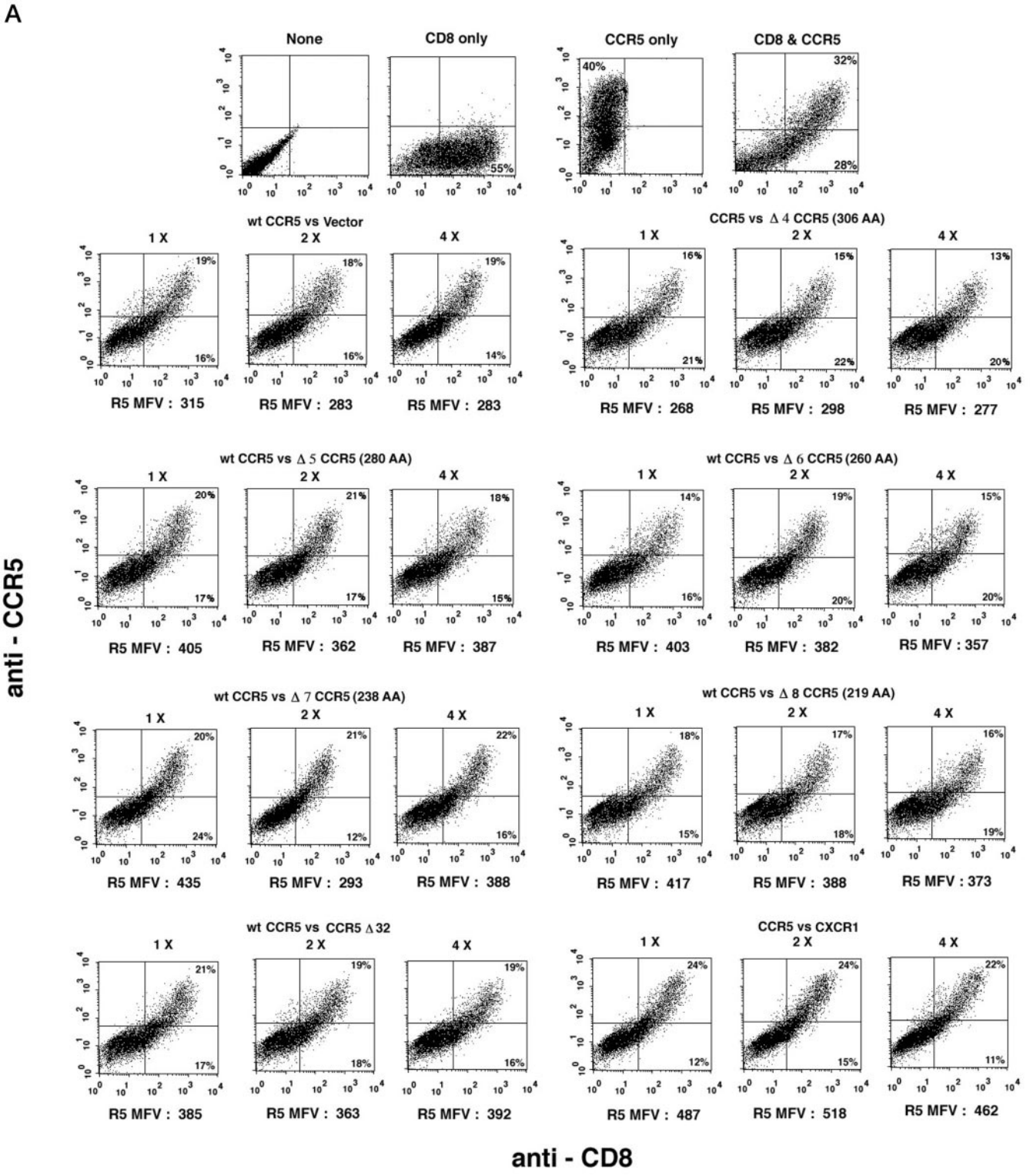

FIG. 5. **Cell surface CCR5 expression is not reduced by the presence of molar excess of transport-impaired CCR5 deletion mutants.** *A*, FACS analysis of cell surface expression of CCR5 co-transfected into 293-T cells with increasing amounts of the indicated CCR5 deletion mutants, vector control, or CXCR1. Conditions are described under "Materials and Methods." Cells were stained with a mixture of PE-conjugated CCR5 antibody, 2D7, and APC-conjugated CD8 antibody. Two-color dot blots representing four experiments are shown. All transfections included CD8 to monitor transfection efficiency. Cells transfected with WT CCR5 or CD8 alone and untransfected cells (*mock*), set the controls. Mean fluorescence values (MFVs) of CCR5s were normalized to constant CD8 values and are given *below* each *plot*. *B*, MFVs from all experiments represented by *A* were averaged and presented as a histogram with *error bars*, where the MFV for WT CCR5 was arbitrarily set to 100.

We examined whether more drastic changes such as in Δ8 or CCR5Δ32 might affect protein stability and turnover. 293-T cells were co-transfected with CD8 and the indicated CCR5 plasmids. 10^6 cell aliquots of the indicated transfectants were labeled with [^{35}S]methionine for 30 min, and the cell extracts were immunoprecipitated with rabbit anti-CCR5 antiserum (27). Immunoprecipitates were resolved by SDS-PAGE and visualized by PhosphorImager scanning. The various CCR5 deletion mutants were expressed as well if not better than WT CCR5 (Fig. 4*A*). Cells were analyzed for CD8 expression by

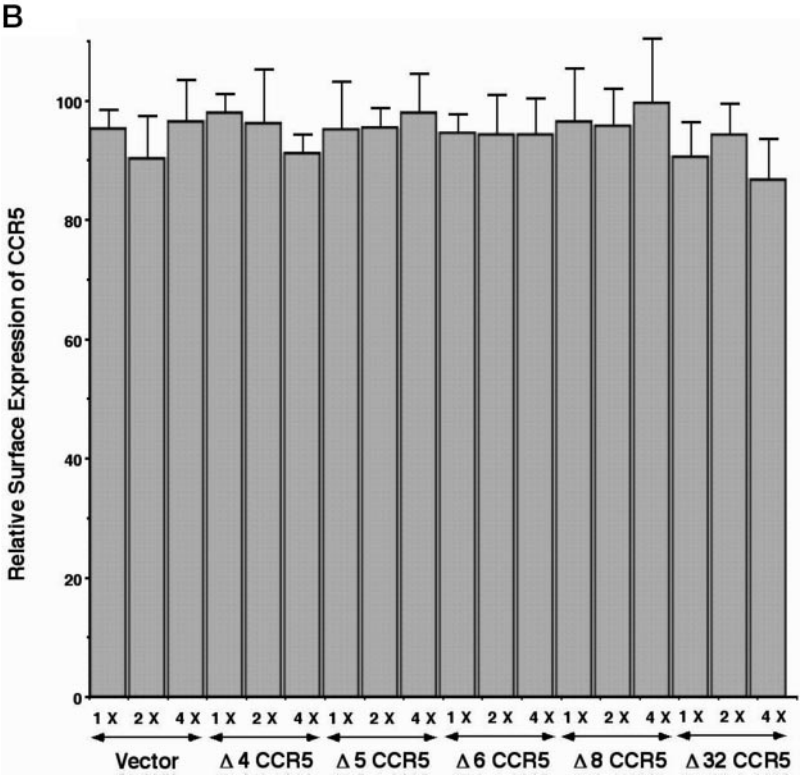

FIG. 5—*continued*

FACS, and individual transfectants were adjusted to constant CD8+ levels. Following a labeling period of 15 min with [^{35}S]methionine, the cells were metabolically "chased" for up to 8 h. CCR5 was immunoprecipitated using a rabbit antiserum raised against the N-terminal peptide of CCR5. Labeled CCR5 was resolved by SDS-PAGE and visualized by radioactivity scanning. The PhosphorImager profile shown in Fig. 4*B* is representative of two experiments. Within 1 h of chase, nascent WT CCR5 was converted to a slowly migrating species, probably representing the *O*-glycosylated form of CCR5 (31). By comparison with WT CCR5, none of the deletion mutants displayed abnormal turnover. As expected, deletion mutants that were retained mostly or exclusively in the ER were not *O*-glycosylated.

Cell Surface CCR5 Expression Is Not Inhibited by a Molar Excess of Transport-impaired CCR5 Deletion Mutants—Having shown that CCR5Δ32 and other C-terminal truncations that were impaired for surface expression accumulated in the ER, we inquired whether they might sequester and inhibit the normal anterograde transport of WT CCR5. Cell surface expression of WT CCR5 in the presence of a molar excess of CCR5 deletion mutants or unrelated CXCR1 or vector DNA was examined following transfection of human epithelial 293-T and HeLa cells and in Jurkat T-lymphocytes. CD8 was co-transfected to normalize for DNA transfer efficiency. Cell surface densities of CD8 and CCR5 were examined by two-color FACS using the respective monoclonal antibodies directly conjugated with nonoverlapping chromophores (*i.e.* FITC and TC or PE and APC). Fig. 5*A* illustrates results obtained with 293-T cells. CD8 or CCR5 surface densities in cells transfected singly with either receptor allowed us to set the expression gates for the respective receptors. A dot plot of cells transfected with WT CCR5 and CD8 showed a double positive diagonal population with almost equivalent staining for both receptors. Events occurring in both the lower and upper right quadrants of individual plots together constitute the transfected population. Mean fluorescence values (MFVs) for CCR5 were computed for the transfected population (gated for CD8) and normalized to constant CD8 values. Co-transfecting vector DNA at different molar ratios over CCR5 resulted in a decrease in the overall transfected population (60% *versus* 35–40%) but did not impact significantly on the MFV for CCR5. Against this backdrop, co-transfection of increasing amounts of CCR5Δ32 and other *in vitro* engineered CCR5 deletion mutants had no significant effects on the surface expression of CCR5. Co-expression of CXCR1 (Fig. 5*A*) or other CC or CXC receptors including CCR2B and CXCR2 (data not shown) did not affect cell surface levels of CCR5. Experiments shown in Fig. 5*A* were repeated four times in 293-T cells, and as shown by the histogram in Fig. 5*B*, the results did not vary by more than 15–20%. CCR5 expression in the presence of a 2-fold molar excess of vector DNA, Δ8, and CCR5Δ32 mutants was analyzed twice with two other CCR5 mAbs (3A9 and 182) and was found to be unaffected (data not shown). Likewise, co-transfection of CCR5 mutants did not affect CCR5 surface expression in HeLa cells ($n = 2$) and COS-1 cells ($n = 1$). With a 6–10-fold excess of CCR5 truncation mutants, 30–50% reduction was observed in the surface expression levels of co-transfected WT CCR5. However, at these high input levels, overall transfection efficiency was compromised as a result of cytotoxicity (data not shown). To examine the possibility that transport-defective CCR5 mutants may hinder WT receptor expression in lymphocytes, we repeated the above co-transfection experiments with selected mutants in Jurkat T lymphocytes (Fig. 6*A*). Averaged MFVs compiled from three separate experiments are illustrated in Fig. 6*B*. As with other cell types, co-transfection of a 4-fold molar excess of CCR5 truncation mutants did not affect CCR5 expression significantly when compared with vector DNA co-transfection.

Δ8 or CCR5Δ32 Does Not Co-localize with WT CCR5 either at the Cell Surface or Intracellularly—Although CCR5 deletion mutants did not impair cell surface expression of co-transfected WT CCR5, it was still possible that they might complex with WT CCR5 during intracellular transport or be co-expressed

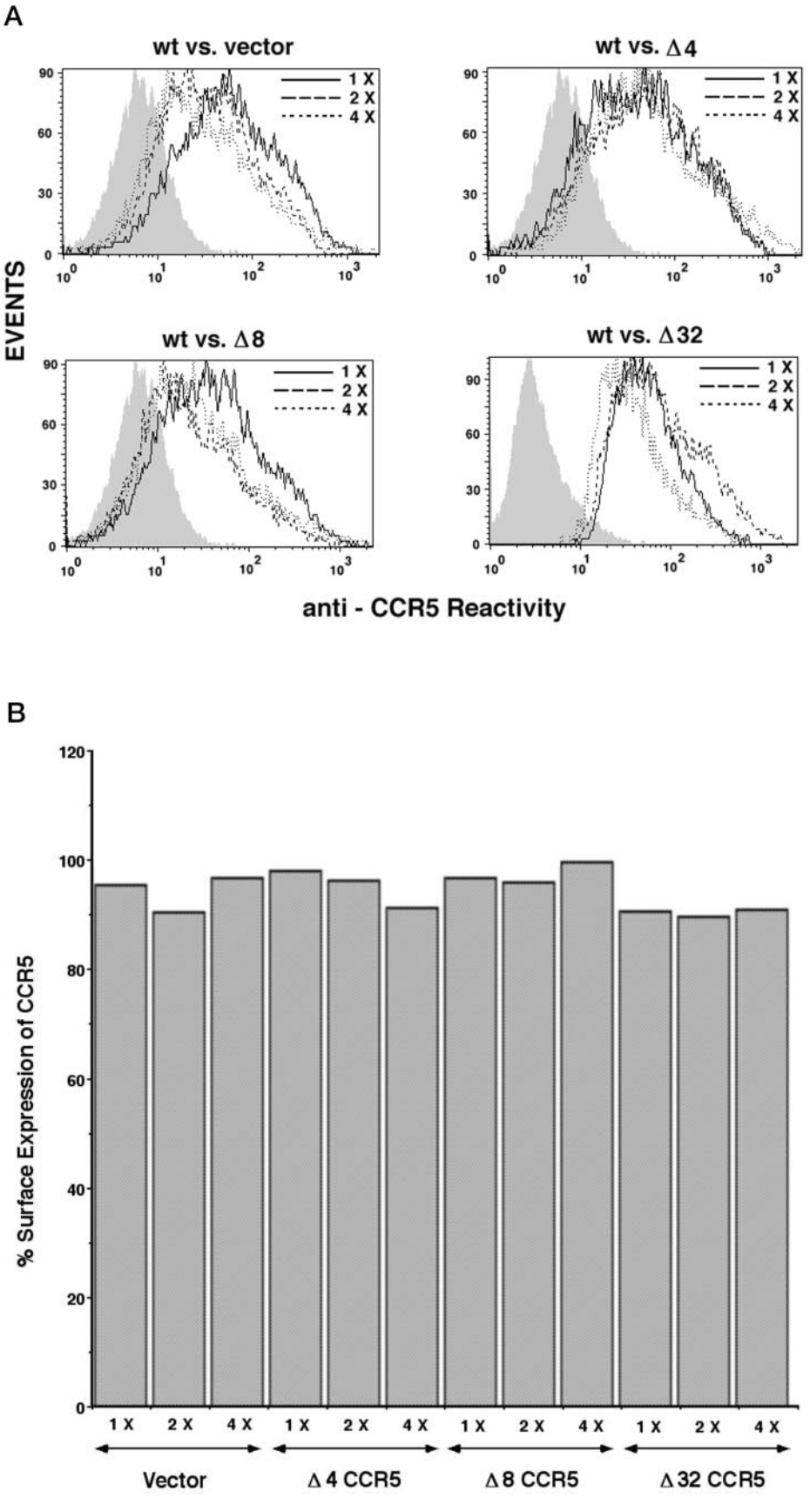

FIG. 6. **Cell surface expression of CCR5 is not impaired by mutant co-expression in Jurkat cells.** Since transfection efficiency of Jurkat cells was typically around 10%, 4×10^5 cells were analyzed and gated for CD8 expression. Cells were stained with a mixture of PE-conjugated anti-CCR5 mAb, 2D7, and APC-conjugated CD8 mAb. *A*, cell surface CCR5 densities in the CD8-gated populations for each set of co-transfectants are plotted in the respective *FACS histogram panels*. Individual plots in each *panel* illustrate results obtained with the designated molar excess of vector DNA or CCR5 mutants over WT CCR5. *B*, averaged MFVs for CCR5 from three experiments are plotted as a *bar diagram*, where WT CCR5 expression level without additional DNAs is set to 100.

with WT receptors at the cell surface as heterodimers. To investigate these scenarios, we co-transfected HeLa cells on coverslips with WT CCR5 and Δ8 or CCR5Δ32 mutants (at a 2.5-fold molar excess of mutant over WT) or vector DNA. Subcellular distribution of WT and mutant CCR5 immunostained on live or fixed and permeabilized cells was examined by confocal microscopy. WT CCR5 was detected by staining with 2D7 or 182 mAb, Δ8 mutant by staining for the FLAG epitope with

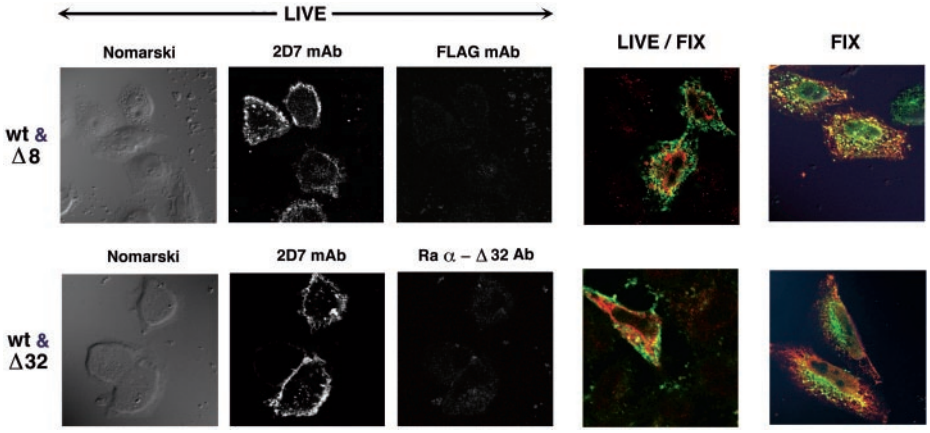

FIG. 7. **Subcellular distribution WT CCR5 co-expressed with the deletion mutant Δ8 or CCR5Δ32.** HeLa cells on 8-mm coverslips were transfected with a mixture of WT CCR5 and Δ8 or CCR5Δ32 DNAs that had a 2.5-fold molar excess of mutant. Transfectants shown in the *FIX panels* were treated with cycloheximide and anisomycin for 30 min prior to antibody staining. Confocal microscopic images are shown. Single channel fluorescence and transmission (Nomarski) images of live cells co-expressing WT and Δ8 or Δ32 CCR5 are shown on the *left* (*LIVE*). 2D7-APC and FLAG-FITC were used for live cells expressing WT and Δ8. Cells were stained with a mixture of 2D7 mAb and rabbit IgG against Δ32 followed by staining with FITC and Texas Red-conjugated second antibodies. In the *LIVE/FIX panel*, WT CCR5 on the cell surface of live cells was stained with APC-conjugated 2D7 mAb (*pseudo-colored green*) followed by extensive washing, fixation, and permeabilization before staining with FITC M2 FLAG mAb or rabbit IgG against Δ32 peptide (*pseudo-colored red*). Rabbit IgG was visualized by staining with Texas Red-conjugated goat anti-rabbit IgG. To examine co-localization of WT and mutant CCR5 inside the cells, transfectants were fixed and permeabilized before staining as above (*FIX*).

unconjugated M2 FLAG mAb, FITC FLAG mAb or rabbit IgG against FLAG peptide, and CCR5Δ32 by staining with a rabbit IgG targeted against the frameshift 33-amino acid sequence of CCR5Δ32. At least eight fields were examined for each coverslip, and the experiment was repeated three times, using in each case different combinations of antibodies and fluorescent chromophores. Live cells expressing WT CCR5 and Δ8 were stained with a mixture of APC-conjugated 2D7 and FITC-conjugated M2 FLAG mAbs. WT CCR5 and CCR5Δ32 co-transfectants were stained with a mixture of unconjugated 2D7 and rabbit IgG against the C terminus of CCR5Δ32, followed by a second staining with a mixture of FITC anti-mouse IgG and Texas Red-conjugated anti-rabbit IgG. The same combination of antibodies was used to stain cells transfected with WT CCR5 and vector DNA. Live transfectants displayed immunoreactivity with WT CCR5-specific mAb but not with Δ8- or CCR5Δ32-specific reagents (Fig. 7, *LIVE*). There was no significant difference in the number of live cells staining positive for CCR5 among cells transfected with WT CCR5 alone or with a mixture of WT CCR5 and mutant(s) or control DNA. In the *panel* to the *right* (*LIVE/FIX*) are shown results obtained when the co-transfectants were sequentially stained, first to display cell surface CCR5 on living cells. Cells were then extensively rinsed, fixed, and permeabilized before staining for Δ8 with FITC FLAG M2 mAb and for CCR5Δ32 with rabbit IgG against CCR5Δ32-specific peptide. Prior to staining receptors in the fixed and permeabilized cells (*FIX panel*), the transfectants were treated with a mixture of cycloheximide (50 μg/ml) and anisomycin (25 μg/ml) for 30 min to stop protein synthesis and induce clearing of nascent proteins from the ER. WT CCR5 staining (in *green*) was distinct at the cell surface but appeared somewhat puckered (resulting from fixation) rather than smooth as in the *LIVE panel*. CCR5 mutants were visualized inside the cells but were excluded from the cell surface, and there is very little, if any, mixing of colors (Fig. 7). The above findings showed that surface expression of WT receptor was unaffected by the mutants. The segregated distribution of WT and mutant CCR5 implied that the mutant CCR5 was not transported to the cell surface by associating with the WT receptor. Both WT and mutant CCR5 were readily detected inside fixed cells but showed no significant co-localization (Fig. 7, *FIX*). However, there was significant mixing of both WT and mutant proteins in the ER of transfectants that had not been treated with protein synthesis inhibitors (not shown). Intensity of cell surface staining in transfectants that had been fixed and permeabilized was highly variable and showed no correlation with the expression levels of co-transfected Δ8 or CCR5Δ32 mutants. *LIVE/FIX* and *FIX* visualizations also confirmed that most cells positive for WT CCR5 also expressed the mutant receptor(s).

Co-expression of Δ8 or CCR5Δ32 Does Not Alter the Functional Competence of WT CCR5 on the Cell Surface—Although CCR5 mutants did not reduce the surface density of co-expressed WT receptor to any significant extent and did not co-localize with the WT counterpart either at the cell surface or intracellularly, it was possible that they might affect the WT receptor function through direct binding or by subtle interaction(s) with the receptor signaling components. Hence, the ability of WT CCR5 to signal in response to chemokine stimulation was examined in 293-T cells co-transfected with WT CCR5, CD8, and vector DNA or the indicated CCR5 mutants.

First, we measured ligand dependent intracellular Ca^{2+} flux. For this purpose, CCR5 was co-transfected with a 4-fold molar excess of vector or mutant plasmids. After checking an aliquot of 10^5 cells for CD8 expression by FACS analysis, individual samples were adjusted to a constant fraction of CD8+ cells. Approximately 5×10^6 cells were preloaded with FURA-2 and analyzed for intracellular Ca^{2+} flux following the addition of 100 nM RANTES. We have shown before that deletions (like Δ4) that excised the C-tail of CCR5 were negative in this assay (30). Co-transfection of molar excess of Δ4 did not interfere with the RANTES-dependent signaling potential of WT receptor (Fig. 8*A*). Likewise, co-expression of Δ8 or CCR5Δ32 also failed to inhibit signaling by the WT receptor. To exclude the possibility that transfections may have resulted in variability in the viability/metabolic state of cells, we evaluated all transfectants for the magnitude of calcium flux responses to stimulation of endogenous CXCR4 or ATP receptor by their respective cognate ligands, SDF-1α or ATP. In no case did we notice any disparities in the magnitudes of Ca^{2+} flux in response to stimulation of endogenous receptors (data not shown). Transfection efficiency was determined by two-color FACS (as described for Fig. 5), and in all cases shown in Fig. 8*A*, CD4-normalized cell surface CCR5 levels were unaltered. Cell numbers were ad-

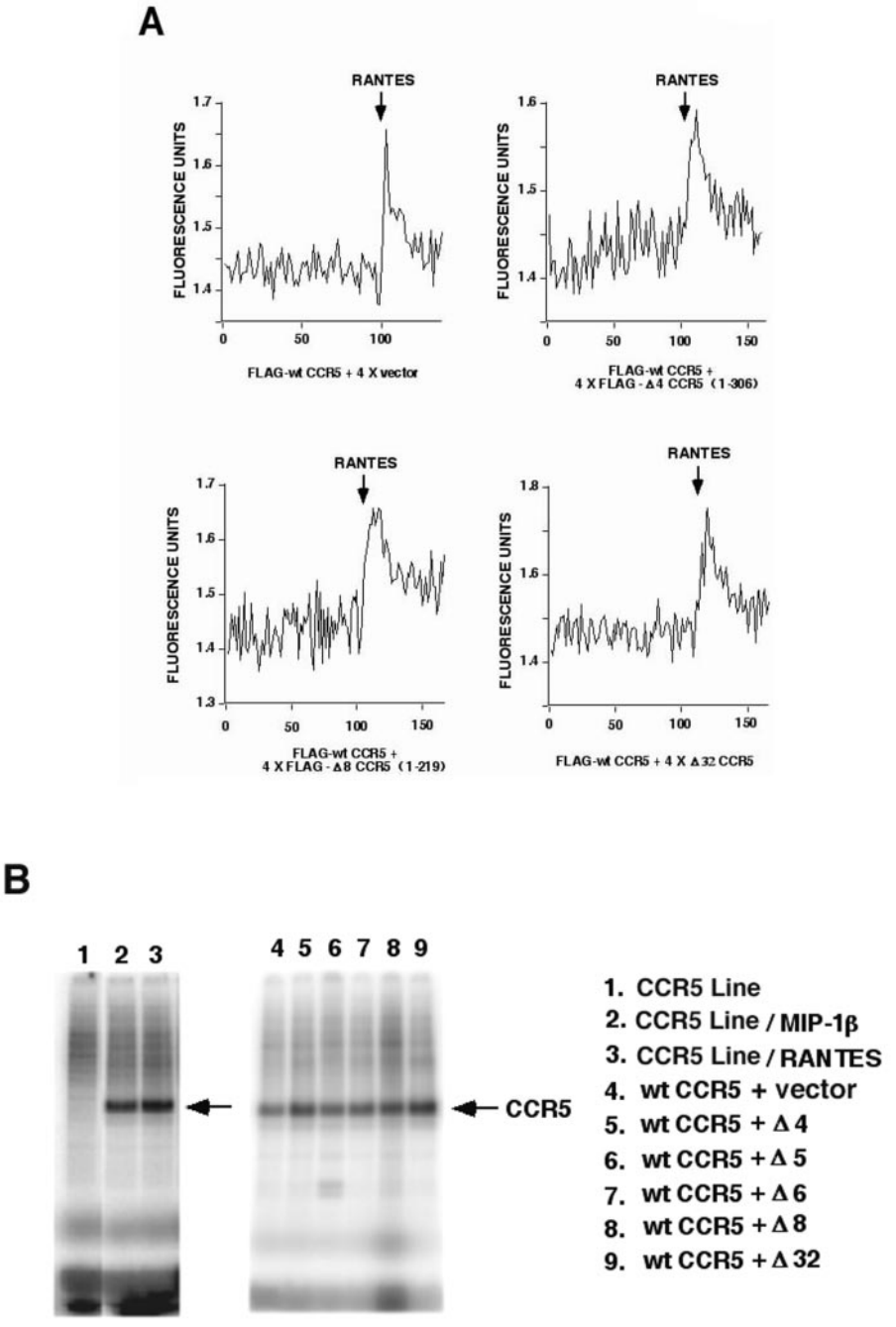

FIG. 8. **Co-expression of CC5 deletion mutants does not alter the functional competence of WT CCR5 on the cell surface.** *A*, signaling potential of 293-T cells co-transfected with WT CCR5 and a 4-fold excess of vector DNA or the indicated CCR5 deletion mutants. Conditions for the CCR5 ligand-dependent Ca^{2+} flux assay are described under "Materials and Methods." Fluorimetric ratios are plotted as a function of time. The *arrows* denote times of addition of RANTES. Plots are representative of three experiments. *B*, a 2-fold molar excess of CCR5 deletion mutants co-expressed with WT CCR5 does not inhibit ligand-dependent phosphorylation of WT CCR5. Conditions of the assay are described under "Materials and Methods." Transfected cell extracts were immunoprecipitated with rabbit IgG against CCR5 N-terminal peptide and resolved by SDS-PAGE followed by PhosphorImager scanning. The scanned gel profile is shown. *Lanes 1–3* represent results obtained with HEK cell line (2×10^6 cells) stably expressing CCR5, while *lanes 4–9* are results obtained with transient transfections. Transfectants were stimulated with RANTES. The experiment was carried out twice and yielded similar results.

justed to constant fraction of CD4+ cells only to adjust for transfection efficiency.

Following ligand binding, GPCRs undergo rapid phosphorylation at serine and/or threonine residues in the C-tail. This early event, catalyzed by the G protein-coupled receptor kinase, leads to receptor desensitization resulting from arrestin mediated receptor endocytosis (32, 33). However, receptor mutants that have lost phosphorylation sites still retain signaling function measured by Ca^{2+} flux (30, 34–36). We inquired whether CCR5 mutants, impaired for surface expression interfered with the ligand-dependent phosphorylation of the WT receptor. 293-T cells were co-transfected with a mixture of CCR5 and CD8 and a 2-fold molar excess of the indicated CCR5 deletion mutants. Following FACS analysis to monitor transfection efficiency, individual transfectants were adjusted to constant levels of CD8+ cells and used in an *in vitro* phosphorylation assay in the presence of RANTES. HEK-293 cells stably expressing WT CCR5 served as positive control. As shown by the PhosphorImager gel profile in Fig. 8*B*, MIP-1β or RANTES stimulation induced phosphorylation of CCR5 (*lanes 2* and *3*). The HEK-293 cell line stably expressing the Δ4 CCR5 mutant was negative in this assay (not shown), resembling the untreated WT CCR5 line (*lane 1*). RANTES-treated parental HEK-293 cells or 293-T cells transfected with Δ8 or CCR5Δ32 mutants or vector DNA were also negative (not shown). Co-transfecting molar excess of different CCR5 deletions including the natural CCR5Δ32 variant (*lanes 5–9*) did not significantly affect the intensity of CCR5 phosphorylation. Further, there was no discernible difference in the metabolic labeling of CCR5 with [^{35}S]methionine (detected by immunoprecipitation) in cells co-transfected with CCR5, CD8 and vector, Δ4, Δ8, or Δ32 plasmids (data not shown). We had already established that the cell surface levels of CCR5 were not modulated by co-expression of vast molar excess of CCR5 mutants (Figs. 5 and

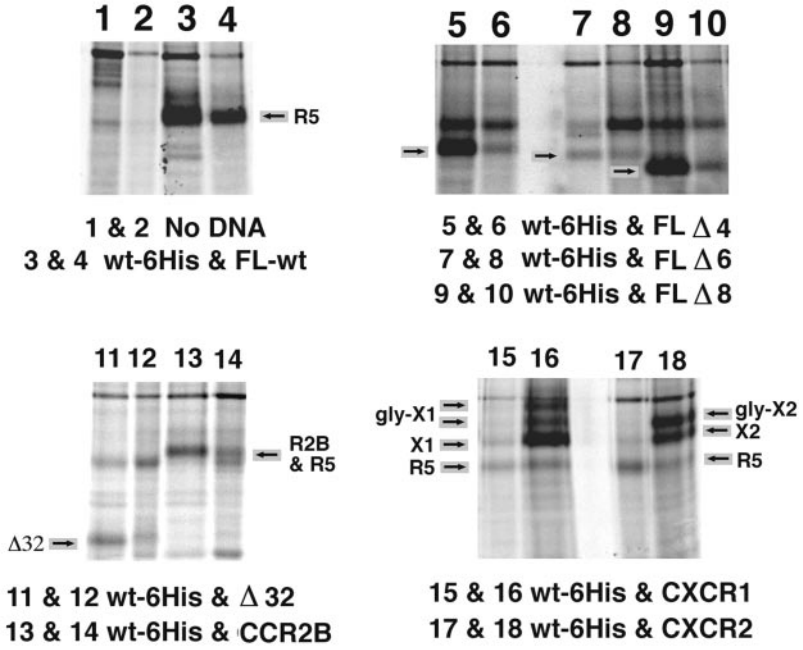

FIG. 9. **Transient intracellular association of WT CCR5 with CCR5 deletion mutants and other CC and CXC chemokine receptors is observed.** 293-T cells were co-transfected with His_6-tagged WT CCR5 (*wt-6His*) and the indicated CCR5 deletion mutants or selected CC and CXC chemokine receptors. CD8 was added to all transfections to normalize for expression efficiency. Transfections were metabolically labeled for 15 min with [^{35}S]methionine, and extracts were prepared. Two equal aliquots of extracts of individual transfectants were immunoprecipitated with the indicated antibodies and run pairwise on SDS-PAGE. PhosphorImager scans are shown. For *lanes 1–10*, FLAG (*odd lanes*) and His_6 (*even lanes*) mAbs were used. For CCR5Δ32 co-transfection, rabbit IgG against CCR5Δ32 fusion peptide (*lane 11*) and His_6 mAb (*lane 12*) were used. For WT His_6 co-transfections with other receptors, *lanes 13*, *15*, and *17* represent results obtained using His_6 mAb. Results obtained using mAbs against CCR2B, CXCR1, and CXCR2 are shown in *lanes 14*, *16*, and *18*. The *unlabeled arrows* in the *top right panel* identify the various CCR5 deletions tagged with the FLAG epitope. The *arrow* to the *left* of *lane 11* denotes CCR5Δ32 protein. The *arrow* to the *right* of *lane 14* identifies co-migrating CCR2B and CCR5 bands. The *arrows* identified as *gly-X1* to the *left* of *lane 15* denote *N*-glycosylated forms of CXCR1 (*gly-X1*), and to the *right* of *lane 18*, *glyX2* refers to the *N*-glycosylated form of CXCR2. The *arrows* labeled *X1* and *X2* identify the unglycosylated CXCR1 and CXCR2, respectively.

6). The signaling experiments described in the legend to Fig. 8, *A* and *B*, emphasized that the functional potential of cell surface CCR5 in the various co-transfectants was also unaltered.

Transient Intracellular Association of WT CCR5 with CCR5 Truncation Mutants and Other CC and CXC Chemokine Receptors—Using a yeast two-hybrid system, Benkirane *et al.* demonstrated physical association of CCR5 with itself or CCR5 deletion mutants including CCR5Δ32 (20). We evaluated this property in transfected 293-T cells under transient labeling conditions. 293-T cells were co-transfected with WT CCR5-His_6 and various CCR5 deletions tagged at the N termini with FLAG epitope. Tranfectants were metabolically labeled with [^{35}S]methionine, and cytoplasmic extracts were immunoprecipitated with His_6 or FLAG mAb in a pairwise manner and analyzed by SDS-PAGE under reducing conditions. As shown in Fig. 9, both FLAG and His_6 mAbs co-precipitated WT-His_6 with the respective FLAG-tagged deletion mutants (*lanes 3–10*). The relative levels of WT-His_6 and the deletion mutants in the co-precipitates were variable, but the pattern shown in Fig. 9 was reproduced in two additional experiments. Similarly, CCR5Δ32 was co-precipitated with WT-His_6 (*lanes 11* and *12*) in two separate experiments. We then inquired whether the mutual co-precipitation was restricted to CCR5 derivatives or whether CCR5 could associate with other CKRs. We examined co-precipitation of CCR5 with CCR2B (*lanes 13* and *14*), CXCR1 (*lanes 15* and *16*), and CXCR2 (*lanes 17* and *18*). In all three cases, there was definite evidence for physical association between nascent CCR5 and the indicated CKRs. Although the relative magnitudes of other CKRs co-precipitated with WT CCR5-His_6 (*lanes 13*, *15*, and *17*) were less than those of CCR5 deletion mutants, the pattern was consistent in three experiments. Also, mAbs against other CKRs were more efficient in co-precipitating CCR5 (*lanes 14*, *16*, and *18*) than vice versa.

M-tropic HIV Usage of WT CCR5 Is Not Impaired by Co-expression of Δ8 or CCR5Δ32—CCR5 expression levels both in PBMCs and cell lines affect the magnitude of M-tropic HIV entry. Naturally occurring Δ32/Δ32 homozygous T cells are resistant to M-tropic virus entry (15–17), while WT/Δ32 heterozygotes display variable reductions in HIV entry (15, 17, 22). Using an indicator HeLa CD4/long terminal repeat-β-galactosidase cell line system, Benkirane *et al.* (20) showed that overexpression of natural CCR5Δ32 or engineered deletions that excised one or two distal TM domains inhibited M-tropic virus entry in a single cycle replication assay. We have shown here that overexpression of CCR5 deletion mutants was largely ineffective in reducing cell surface expression or signaling potential of WT CCR5. We examined M-tropic virus entry more directly and quantitatively using *luc*-expressing HIVs pseudotyped with the M- or T-tropic envelope proteins as described under "Materials and Methods." Results from four experiments are summarized in Table I. 293-T cells were transfected with the indicated combinations of WT CCR5 and vector or mutant CCR5 along with wtCD4 or tailless CD4 (tCD4). Individual transfections of each experiment were monitored for CD4 and CCR5 expression by two-color FACS analysis. There was no significant down-modulation of CCR5 in any of the co-transfectants. Untransfected cells supported only AMLV pseudotyped virus infection. To facilitate quantitative comparison of various infections, AMLV pseudotyped virus infection was performed on transfected cells prior to selection on CD4 immune beads, and the resulting luciferase values were adjusted to a constant number for each experiment. After immune selection, individual transfections were adjusted to con-

TABLE I
Luciferase assay results

Luciferase assay results represent the average of three measurements and are expressed in arbitrary machine units (see "Materials and Methods"). NO, background values when no virus was used; NL, T-tropic NL4–3 HIV; AD and JRFL, the respective eponymous M-tropic HIVs; AMLV, amphotropic murine leukemia virus.

	Relative light units				
	NO	NL	AD	JRFL	AMLV
Expt. 1					
Mock Tfx	36	15	28		9600
tCD4 + CCR5 + vector	68	5315	2875		9600
tCD4 + CCR5 + Δ4	96	5565	1988		9600
tCD4 + CCR5 + Δ8	66	7444	2194		9600
tCD4 + CCR5 + Δ32	17	6369	2012		9600
Expt. 2					
Mock Tfx	5	58		13	12,000
tCD4 + CCR5 + vector	2	4122		3200	12,000
tCD4 + CCR5 + Δ4	12	3898		2630	12,000
tCD4 + CCR5 + Δ8	17	4478		3650	12,000
tCD4 + CCR5 + Δ32	4	3662		2870	12,000
tCD4 + CCR5 + CXCR1	11	4382		3800	12,000
Expt. 3					
Mock Tfx	28	14	22		17,000
CD4 + CCR5 + vector	43	5871	2926		17,000
CD4 + CCR5 + Δ4	80	3108	2670		17,000
CD4 + CCR5 + Δ8	14	4272	3414		17,000
CD4 + CCR5 + Δ32	11	5350	3210		17,000
Expt. 4					
Mock Tfx	54	33	62	42	13,300
CD4 + CCR5 + vector	66	4125	3387	4588	13,300
CD4 + CCR5 + Δ4	18	5287	4125	3785	13,300
CD4 + CCR5 + Δ8	28	3788	3818	3650	13,300
CD4 + CCR5 + Δ32	11	4740	3151	4125	13,300

tain a constant fraction of CD4+ cells prior to infection with the indicated M- or T-tropic Env pseudotyped HIVs. Luciferase expression values were normalized to the constant values obtained with AMLV infection. T-tropic HIV pseudotyped virus (NL) was somewhat more efficient than the M-tropic (AD or JRFL) counterparts. The Δ4 mutant (equivalent to the Δcyt mutant described in Refs. 18 and 19) did not reduce the magnitude of M- or T-tropic virus entry. Consistent with our results on surface expression, co-transfecting a molar excess of either the CCR5Δ32 or the Δ8 mutant also did not reduce the infection by M-tropic HIVs.

CCR5 Expression in PBMCs from CCR5Δ32 Homozygous Individuals—We evaluated steady state levels of CCR5 on PBMCs during *in vitro* T cell activation. Six homozygous WT, six *ccr5Δ32* heterozygotes, and two *ccr5Δ32* homozygotes were chosen. For fresh samples, buffy coats were selected for CD4 and CD45 Ro expression to maximize analysis of long term memory cells. CCR5 levels for this subpopulation were recorded. PBMCs were then purified and activated by CD3 stimulation, and CCR5 levels were determined as described in the legend for Fig. 10. We observed a 2–3-fold difference in CCR5 expression between WT and *CCR5wt/ccr5Δ32* heterozygous subjects (Fig. 10). However, individual variability (*error bars*) in CCR5 levels within each group was greater than the absolute differences in receptor density. Some of these primary T cells were analyzed for virus entry, and M-tropic HIV entry levels did not vary by more than 50% between the WT subject with maximal CCR5 and *CCR5wt/ccr5Δ32* heterozygotes with the minimal receptor density (not shown).

DISCUSSION

In this paper, we evaluated the effects of CCR5Δ32 or other engineered deletion mutants on cell surface density, functional potential, and M-tropic HIV co-receptor usage of co-expressed WT receptor. Contrary to published reports, we found that WT CCR5 expression and function were unaffected by the presence of mutant receptors. Our conclusions are based on 1) FACS analysis showing lack of a significant effect on the steady-state cell surface density of WT CCR5 by the presence of CCR5 mutants under transient expression conditions that controlled for transfection efficiency in human epithelial and Jurkat T cells; 2) simultaneous confocal microscopic visualization of WT and CCR5 mutants expressed in the same cells that showed clear segregation of WT CCR5 and mutant receptor; 3) unaltered intracellular signaling by WT CCR5 in the presence of CCR5 truncation mutants; and 4) lack of significant effects by CCR5 deletion mutants on the magnitude of M-tropic HIV entry of purified cells expressing WT CCR5 and CD4.

Under steady-state conditions, the cell surface density of WT CCR5 or co-expressed CD8 control was unaffected by a 4-fold molar excess of mutant receptor plasmids in HEK-293 or Jurkat T cells. This is in direct contrast with the results of Shioda *et al.* (19), who showed that *CCR5-893*(−) mutant severely reduced the surface expression of WT receptor. This was demonstrated by FACS analysis of Jurkat cells co-infected with recombinant Sendai virus expressing WT and mutant CCR5. However, the effect of infection by multiple Sendai viruses on delivered antigen expression was not controlled for, making interpretation of the results difficult. From the FACS histogram of the ungated population showing staining results from an FITC-conjugated second IgG, it was difficult to assess the contribution of nonspecific staining. The *CCR5-893*(−) mutant is similar to our Δ4 mutant, except that Δ4 has 7 residues of authentic CCR5 sequence in the C-terminal domain, while *CCR5-893*(−) has 10 unnatural residues encoded by the −1 frame. We have shown by multiple criteria that Δ4 had no effect on the functional expression of WT CCR5 at the cell surface. However, it is possible that the 10 incorrect amino acids added to the C terminus of *CCR5-893*(−) could affect WT CCR5 expression.

High resolution confocal microscopic visualization of immunostained HeLa co-transfectants established that WT CCR5, but not the deletion mutants, was present at the cell surface. Live cells co-transfected with WT and mutant CCR5 displayed WT but not the mutant receptors at the cell surface when

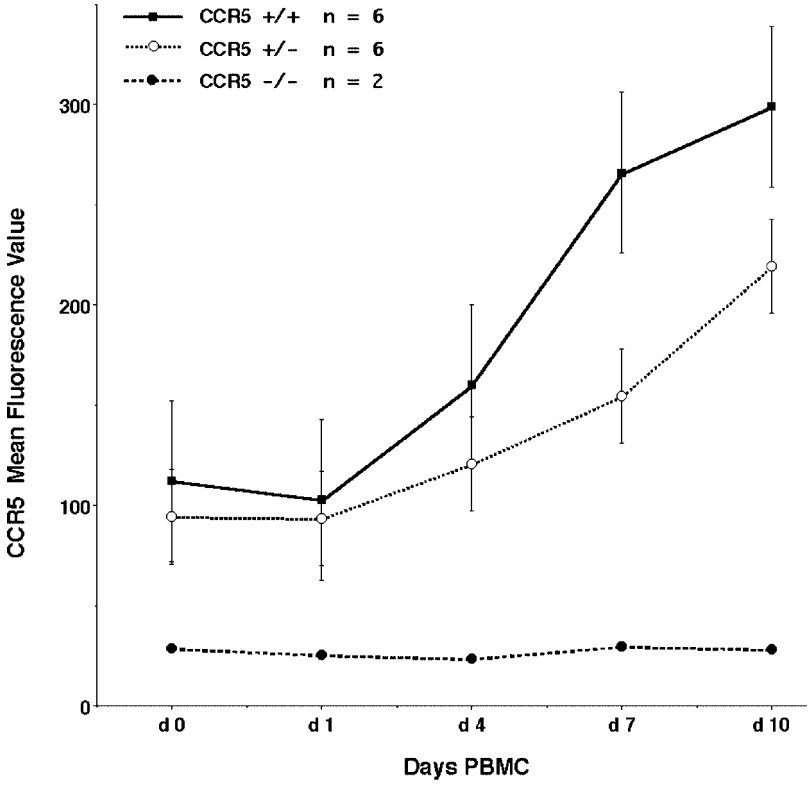

FIG. 10. **Time course of CCR5 expression in PBMCs with WT homo- or heterozygotic Δ32 alleles.** PBMCs from volunteers were analyzed for CCR5 expression by flow cytometry during *in vitro* activation by antibody cross-linking of CD3 receptor. For day 0 (*d0*), buffy coat was used directly without centrifugal purification using lymphocyte separation medium. Samples corresponding to days 0 and 1 were stained for CD4, CD45-RO, and CCR5. Significant CCR5-positive cells were identified only in the CD4+/CD45-RO+ gated population. For days 1 and 4, CCR5 values were determined for the CD4+ and CD4+/CD25+ subpopulations. For days 7 and 10, CCR5 levels were determined for the CD4+ population. Average CCR5 MFVs are plotted with *error bars* as a function of time. *n* refers to the number of samples studied.

several fields were examined in three independent experiments using different combinations of antibodies and fluorescent chromophores. By simultaneous visualization of WT receptor in living cells and the mutant(s) after fixation and permeabilization, we showed that WT receptor levels at the cell surface were not diminished by production of mutant receptor. In contrast to the previous report of Benkirane *et al.* (20), WT CCR5 did not show any significant co-localization with the Δ8 or CCR5Δ32 mutants (20). The earlier observations probably reflected mixing of the nascent receptors, the ER, since we noticed similar co-localization of receptors in the ER when protein synthesis was not arrested in the transfectants.

Functional integrity of cell surface CCR5 in the context of overexpression of mutant receptors was examined by three different assays. A molar excess of mutant receptors did not significantly affect the ability of co-expressed WT CCR5 to support M-tropic virus entry. Our results were in discord with the Benkirane *et al.* report (20) that demonstrated marked diminution of M-tropic HIV infection of cells co-expressing WT CCR5 and a molar excess of CCR deletion mutants including CCR5Δ32. Our assay relied on a quantitative luciferase-based assay rather than the MAGI assay used by Benkirane *et al.* (20). Although the two assays differ in their quantitation and subjectivity, both of them measure single cycle HIV replication. In the MAGI assay, HIV Tat-driven transcription of long terminal repeat-linked β-galactosidase in HeLa CD4 cells served as the barometer of infection with T- or M-tropic HIV. We generated pseudotyped HIVs carrying the *luc* gene in place of Nef to infect transient transfectants expressing various combinations of WT and mutant CCR5 in addition to CD4. HIV entry was measured by assaying for Tat-driven luciferase expression from the integrated provirus following virus entry. Transient transfection of both CD4 and CCR5 enabled us to monitor the simultaneous expression of both receptors by FACS and verify that CCR5 expression was not adversely influenced by co-expression of CCR5 mutant(s), which was not done in the earlier report (20). Therefore, the relative ratios of CCR5 and CD4 levels were already known in the CD4+ cells purified to near homogeneity from individual transfections before virus adsorption. AMLV Env pseudotyped HIV infection of unselected cells provided a suitable yardstick for quantitative comparison of T- and M-tropic virus entry. This was in contrast to the earlier work that used HeLa CD4 MAGI cells for M-tropic HIV entry without correlation with CCR5 expression (20). Previous work on threshold requirements of CCR5 for M-tropic HIV entry has emphasized the importance of relative ratios of CD4 and CCR5 (37). Microscopic enumeration of β-galactosidase positive foci without normalizing for transfection variability did not take this into account. Further, HeLa CD4 cells express CXCR4 constitutively; therefore, a substantial fraction, if not all of them, should have been susceptible to T-tropic HIV infection, but the authors did not provide any quantitative comparisons. Further, we compared replication potential of two M-tropic strains (JRFL and AD88) with that of the T-tropic NL4-3 strain in transfectants expressing WT or tailless CD4. A 6–10-fold excess of CCR5Δ32 that resulted in 30–50% reduction in cell surface CCR5 may have reduced the magnitude of M-tropic virus entry. However, effects on virus infection at high DNA inputs could not be assessed because of poor cell viability. Considering the low threshold levels of CCR5 for HIV entry, it is unlikely that a modest decrease in the cell surface levels of CCR5 would have resulted in a corresponding decrease in virus susceptibility. Although the mutant receptors neither reduced the cell surface levels of WT CCR5 nor were present on the cell surface complexed with CCR5, it was formally possible that the mutants might have subverted the intracellular pathways pertaining to chemokine signaling by the WT receptor. Using two biochemical assays for ligand-dependent CCR5 signaling, intracellular Ca^{2+} flux, and receptor phosphorylation, we showed that the mutants caused no perturbation in the WT receptor function.

Receptor dimerization is an intrinsic property of some, but not all GPCRs. Some, such as metabotropic glutamate receptors, exist as covalent dimers, disulfide-linked through their

long N termini (38–40). In the case of γ-aminobutyric acid type B-1 receptors, heterodimerization is required for functional surface expression (41). Other studies have found that agonist binding may increase (42–44), decrease (45, 46), or cause no change in dimer levels (47, 48). Heterodimerization between related subunits of GPCRs may alter or expand ligand specificity (45), and some may function as oligomers *in vivo* (48). Among human CKRs, both CCR2 and CCR5 have been shown to form dimers upon ligand binding (43, 49), and CCR5 dimerization has been presumed to modulate HIV entry (49) and T cell activation through the Jak signaling pathway (50). Ligand- or antibody-induced CCR5 dimerization (49) and heterodimerization of CCR5 or CXCR4 with a natural CCR2 mutant allele, CCR2-V64I (51), have been proposed to hinder HIV infection. Using a yeast two-hybrid system, Benkirane *et al.* (20) demonstrated that CCR5 formed dimers through sequence spanning the N terminus and the first TM domain. This was consistent with results from our co-precipitation experiments. CCR5 associated with the deletion mutants during transient labeling of nascent molecules. But we demonstrated similar association between CCR5 and CCR2B, CXCR1, or CXCR2, albeit to a lesser extent. Further, it was not clear whether the interaction between WT and mutant CCR5 persisted throughout intracellular transport and surface expression of CCR5. Co-precipitation of receptors during metabolic chase of pulse-labeled transfectants was inconsistent and inefficient, partly because of variable turnover rates obtained with epitope-specific mAbs. However, using confocal microscopy, we have shown that in the steady state, WT and truncated receptors segregated into distinct nonoverlapping subcellular compartments.

Inefficient processing, ER retention, and subsequent degradation of misfolded proteins are hallmarks of biogenesis of many GPCRs, particularly in an unnatural cellular context (52–55). Functionally defective, naturally occurring mutations in GPCRs including CCR5 exhibit impaired processing and intracellular retention (56–59). Although exact mechanisms responsible for cytoplasmic retention are not known, one scenario would be that in the absence of positive regulators of transport, oligomerization of TM domains of these proteins may trap them in the ER or the Golgi apparatus (20, 60). However, it must be noted that for many members of GPCRs, receptor dimerization is of paramount physiological significance regulating such processes as ligand selection, signal transduction, receptor trafficking, etc. (61–65). Given this scenario, it is not unusual to expect that mutant receptors can sequester their WT counterparts in the cytoplasm by heterodimer formation. Such a phenomenon has been described for GPCRs of neurotransmitter ligands, exemplified by the V2 vasopressin receptor. Truncated V2 receptor mutants act as negative regulators of WT V2 receptor function (60). We showed previously that CCR5 transport to the cell surface was not as efficient as that of other CKRs and was governed by the presence of several sequence elements in the C-terminal tail of CCR5 (30). We have shown here and elsewhere that unlike some other GPCRs, transport-defective CCR5 mutants were not aberrantly degraded (30). However, in transient expression systems, not all of the *de novo* synthesized CCR5 may be properly assembled and transported to the cell surface, as is the case for other receptors (52, 53) and viral glycoproteins (66). This would leave a fraction of unprocessed receptor in the ER ready to commingle with the transport-impaired mutants. At a 6–10-fold molar excess of CCR5Δ32 or Δ8 plasmid input over that of WT CCR5, we observed a 30–50% reduction in the cell surface density of WT CCR5, which may have reflected a corresponding increase in the size of the unprocessed pool of WT CCR5. The CCR5 complexes we detected in the transient expression system may reflect this residual pool that may not be quantitatively important or physiologically relevant. The CCR5 interactions scored in the yeast two-hybrid system and mapped to the N terminus and the first TM domain of the receptor (20) may still be relevant for agonist selection and binding affinity at the cell surface, as suggested by the mutant phenotype in these domains (67).

Our findings that a molar excess of CCR5Δ32 mutant did not inhibit WT receptor expression may be extrapolated to the role of this allele in *CCR5/ccr5Δ32* heterozygous subjects. Immunophenotyping of a large number of matched WT and heterozygous subjects had suggested that despite individual variability, CCR5 density on PBMCs from *CCR5/ccr5Δ32* heterozygous subjects was reduced more than could be accounted for by halving of the gene dose (17). Using a limited set of matched subjects, we could detect no more than a 2–3-fold difference in CCR5 expression between WT heterozygotic PBMCs during 10 days of culture (Fig. 10). Our findings are in good agreement with the recent reports showing a similar difference in CCR5 levels in PBMCs from WT and CCR5Δ32 heterozyogotes (21, 68). Minimal threshold CCR5 levels for productive HIV infection of PBMCs are largely unknown, since *in vivo* levels of CCR5 on circulating PBMCs may be modulated by many unidentified factors relating to immune challenge and inflammation. Threshold levels of CCR5 for virus infection may be lower than minimal levels required for detection by mAb binding or chemokine response (data not shown). At these levels, reduced gene dosage, rather than dominant interference by the product of the mutant allele may determine HIV susceptibility in the *CCR5/ccr5Δ32* and the *CCR5-893*(−) heterozygous subjects.

Acknowledgments—We thank Alicia Buckler-White of NIAID, National Institutes of Health, for oligonucleotide synthesis. We thank Jan Lukszo of the Peptide Synthesis Unit, RTB, NIAID for the peptides. We thank Owen Schwartz of the Biological Imaging Facility, RTB, NIAID for technical advice on the use of the confocal microscope. We thank Bernard M. Moss of NIAID and John Hanover of NIDDK for critical review and comments. We are grateful to Nelson Cole of HGRI, National Institutes of Health, for supplying Deng antibody reactive with Golgi apparatus and acknowledge the contribution of several reagents by the National Institutes of Health AIDS Research and Reference Reagent Program (Rockville, MD).

REFERENCES

1. Baldwin, J. M., Schertler, G. F., and Unger, V. M. (1997) *J. Mol. Biol.* **272,** 144–164
2. Ji, T. H., Grossmann, M., and Ji, I. (1998) *J. Biol. Chem.* **273,** 17299–17302
3. Wess, J. (1997) *FASEB J.* **11,** 346–354
4. Alkhatib, G., Combadiere, C., Broder, C. C., Feng, Y., Kennedy, P. E., Murphy, P. M., and Berger, E. A. (1996) *Science* **272,** 1955–1958
5. Deng, H., Liu, R., Ellmeier, W., Choe, S., Unutmaz, D., Burkhart, M., Di Marzio, P., Marmon, S., Sutton, R. E., Hill, C. M., Davis, C. B., Peiper, S. C., Schall, T. J., Littman, D. R., and Landau, N. R. (1996) *Nature* **381,** 661–666
6. Doranz, B. J., Rucker, J., Yi, Y., Smyth, R. J., Samson, M., Peiper, S. C., Parmentier, M., Collman, R. G., and Doms, R. W. (1996) *Cell* **85,** 1149–1158
7. Dragic, T., Litwin, V., Allaway, G. P., Martin, S. R., Huang, Y., Nagashima, K. A., Cayanan, C., Maddon, P. J., Koup, R. A., Moore, J. P., and Paxton, W. A. (1996) *Nature* **381,** 667–673
8. Combadiere, C., Ahuja, S. K., Tiffany, H. L., and Murphy, P. M. (1996) *J. Leukocyte Biol.* **60,** 147–152
9. Locati, M., and Murphy, P. M. (1999) *Annu. Rev. Med.* **50,** 425–440
10. Berger, E. A., Doms, R. W., Fenyo, E. M., Korber, B. T., Littman, D. R., Moore, J. P., Sattentau, Q. J., Schuitemaker, H., Sodroski, J., and Weiss, R. A. (1998) *Nature* **391,** 240
11. Arenzana-Seisdedos, F., Virelizier, J. L., Rousset, D., Clark-Lewis, I., Loetscher, P., Moser, B., and Baggiolini, M. (1996) *Nature* **383,** 400
12. Cocchi, F., DeVico, A. L., Garzino-Demo, A., Arya, S. K., Gallo, R. C., and Lusso, P. (1995) *Science* **270,** 1811–1815
13. Bleul, C. C., Farzan, M., Choe, H., Parolin, C., Clark-Lewis, I., Sodroski, J., and Springer, T. A. (1996) *Nature* **382,** 829–833
14. Oberlin, E., Amara, A., Bachelerie, F., Bessia, C., Virelizier, J. L., Arenzana-Seisdedos, F., Schwartz, O., Heard, J. M., Clark-Lewis, I., Legler, D. F., Loetscher, M., Baggiolini, M., and Moser, B. (1996) *Nature* **382,** 833–835
15. Dean, M., Carrington, M., Winkler, C., Huttley, G. A., Smith, M. W., Allikmets, R., Goedert, J. J., Buchbinder, S. P., Vittinghoff, E., Gomperts, E., Donfield, S., Vlahov, D., Kaslow, R., Saah, A., Rinaldo, C., Detels, R., and O'Brien, S. J. (1996) *Science* **273,** 1856–1862
16. Huang, Y., Paxton, W. A., Wolinsky, S. M., Neumann, A. U., Zhang, L., He, T., Kang, S., Ceradini, D., Jin, Z., Yazdanbakhsh, K., Kunstman, K., Erickson,

D., Dragon, E., Landau, N. R., Phair, J., Ho, D. D., and Koup, R. A. (1996) *Nat. Med.* **2,** 1240–1243
17. Wu, L., Paxton, W. A., Kassam, N., Ruffing, N., Rottman, J. B., Sullivan, N., Choe, H., Sodroski, J., Newman, W., Koup, R. A., and Mackay, C. R. (1997) *J. Exp. Med.* **185,** 1681–1691
18. Ansari-Lari, M. A., Liu, X. M., Metzker, M. L., Rut, A. R., and Gibbs, R. A. (1997) *Nat. Genet.* **16,** 221–222
19. Shioda, T., Nakayama, E. E., Tanaka, Y., Xin, X., Liu, H., Kawana-Tachikawa, A., Kato, A., Sakai, Y., Nagai, Y., and Iwamoto, A. (2001) *J. Virol.* **75,** 3462–3468
20. Benkirane, M., Jin, D. Y., Chun, R. F., Koup, R. A., and Jeang, K. T. (1997) *J. Biol. Chem.* **272,** 30603–30606
21. Paxton, W. A., Kang, S., Liu, R., Landau, N. R., Gingeras, T. R., Wu, L., Mackay, C. R., and Koup, R. A. (1999) *Immunol. Lett.* **66,** 71–75
22. Zimmerman, P. A., Buckler-White, A., Alkhatib, G., Spalding, T., Kubofcik, J., Combadiere, C., Weissman, D., Cohen, O., Rubbert, A., Lam, G., Vaccarezza, M., Kennedy, P. E., Kumaraswami, V., Giorgi, J. V., Detels, R., Hunter, J., Chopek, M., Berger, E. A., Fauci, A. S., Nutman, T. B., and Murphy, P. M. (1997) *Mol. Med.* **3,** 23–36
23. Marmor, M., Sheppard, H. W., Donnell, D., Bozeman, S., Celum, C., Buchbinder, S., Koblin, B., and Seage, I. G. (2001) *J. Acquired Immune Defic. Syndr.* **27,** 472–481
24. Liu, R., Paxton, W. A., Choe, S., Ceradini, D., Martin, S. R., Horuk, R., MacDonald, M. E., Stuhlmann, H., Koup, R. A., and Landau, N. R. (1996) *Cell* **86,** 367–377
25. Ahuja, S. K., Lee, J. C., and Murphy, P. M. (1996) *J. Biol. Chem.* **271,** 225–232
26. Alkhatib, G., Berger, E. A., Murphy, P. M., and Pease, J. E. (1997) *J. Biol. Chem.* **272,** 20420–20426
27. Alkhatib, G., Locati, M., Kennedy, P. E., Murphy, P. M., and Berger, E. A. (1997) *Virology* **234,** 340–348
28. Combadiere, C., Ahuja, S. K., and Murphy, P. M. (1996) *J. Biol. Chem.* **270,** 16491–16494; Correction (1997) *J. Biol. Chem.* **271,** 11034
29. Venkatesan, S., Gerstberger, S. M., Park, H., Holland, S. M., and Nam, Y. (1992) *J. Virol.* **66,** 7469–7480
30. Venkatesan, S., Petrovic, A., Locati, M., Kim, Y.-O., Weissman, D., and Murphy, P. M. (2001) *J. Biol. Chem.* **276,** 40133–40145
31. Farzan, M., Mirzabekov, T., Kolchinsky, P., Wyatt, R., Cayabyab, M., Gerard, N. P., Gerard, C., Sodroski, J., and Choe, H. (1999) *Cell* **96,** 667–676
32. Zhang, J., Ferguson, S. S., Barak, L. S., Aber, M. J., Giros, B., Lefkowitz, R. J., and Caron, M. G. (1997) *Receptors Channels* **5,** 193–199
33. Ferguson, S. S. (2001) *Pharmacol. Rev.* **53,** 1–24
34. Krupnick, J. G., and Benovic, J. L. (1998) *Annu. Rev. Pharmacol. Toxicol.* **38,** 289–319
35. Oppermann, M., Mack, M., Proudfoot, A. E., and Olbrich, H. (1999) *J. Biol. Chem.* **274,** 8875–8885
36. Pitcher, J. A., Freedman, N. J., and Lefkowitz, R. J. (1998) *Annu. Rev. Biochem.* **67,** 653–692
37. Platt, E. J., Wehrly, K., Kuhmann, S. E., Chesebro, B., and Kabat, D. (1998) *J. Virol.* **72,** 2855–2864
38. Kunishima, N., Shimada, Y., Tsuji, Y., Sato, T., Yamamoto, M., Kumasaka, T., Nakanishi, S., Jingami, H., and Morikawa, K. (2000) *Nature* **407,** 971–977
39. Romano, C., Miller, J. K., Hyrc, K., Dikranian, S., Mennerick, S., Takeuchi, Y., Goldberg, M. P., and O'Malley, K. L. (2001) *Mol. Pharmacol.* **59,** 46–53
40. Romano, C., Yang, W. L., and O'Malley, K. L. (1996) *J. Biol. Chem.* **271,** 28612–28616
41. White, J. H., Wise, A., Main, M. J., Green, A., Fraser, N. J., Disney, G. H., Barnes, A. A., Emson, P., Foord, S. M., and Marshall, F. H. (1998) *Nature* **396,** 679–682
42. Hebert, T. E., Moffett, S., Morello, J. P., Loisel, T. P., Bichet, D. G., Barret, C., and Bouvier, M. (1996) *J. Biol. Chem.* **271,** 16384–16392
43. Rodriguez-Frade, J. M., Vila-Coro, A. J., de Ana, A. M., Albar, J. P., Martinez, A. C., and Mellado, M. (1999) *Proc. Natl. Acad. Sci. U. S. A.* **96,** 3628–3633
44. Ward, D. T., Brown, E. M., and Harris, H. W. (1998) *J. Biol. Chem.* **273,** 14476–14483
45. Jordan, B. A., and Devi, L. A. (1999) *Nature* **399,** 697–700
46. Gomes, I., Jordan, B. A., Gupta, A., Rios, C., Trapaidze, N., and Devi, L. A. (2001) *J. Mol. Med.* **79,** 226–242
47. Zeng, F. Y., and Wess, J. (1999) *J. Biol. Chem.* **274,** 19487–19497
48. Overton, M. C., and Blumer, K. J. (2000) *Curr. Biol.* **10,** 341–344
49. Vila-Coro, A. J., Mellado, M., Martin de Ana, A., Lucas, P., del Real, G., Martinez, A. C., and Rodriguez-Frade, J. M. (2000) *Proc. Natl. Acad. Sci. U. S. A.* **97,** 3388–3393
50. Rodriguez-Frade, J. M., Vila-Coro, A. J., Martin, A., Nieto, M., Sanchez-Madrid, F., Proudfoot, A. E., Wells, T. N., Martinez, A. C., and Mellado, M. (1999) *J. Cell Biol.* **144,** 755–765
51. Mellado, M., Rodriguez-Frade, J. M., Vila-Coro, A. J., de Ana, A. M., and Martinez, A. C. (1999) *Nature* **400,** 723–724
52. Petaja-Repo, U. E., Hogue, M., Laperriere, A., Walker, P., and Bouvier, M. (2000) *J. Biol. Chem.* **275,** 13727–13736
53. Petaja-Repo, U. E., Hogue, M., Laperriere, A., Bhalla, S., Walker, P., and Bouvier, M. (2001) *J. Biol. Chem.* **276,** 4416–4423
54. Jockers, R., Angers, S., Da Silva, A., Benaroch, P., Strosberg, A. D., Bouvier, M., and Marullo, S. (1999) *J. Biol. Chem.* **274,** 28900–28908
55. Obin, M. S., Jahngen-Hodge, J., Nowell, T., and Taylor, A. (1996) *J. Biol. Chem.* **271,** 14473–14484
56. Nathans, J. (1992) *Biochemistry* **31,** 4923–4931
57. Latronico, A. C., and Segaloff, D. L. (1999) *Am. J. Hum. Genet.* **65,** 949–958
58. Oksche, A., and Rosenthal, W. (1998) *J. Mol. Med.* **76,** 326–337
59. Sung, C. H., Makino, C., Baylor, D., and Nathans, J. (1994) *J. Neurosci.* **14,** 5818–5833
60. Zhu, X., and Wess, J. (1998) *Biochemistry* **37,** 15773–15784
61. Hebert, T. E., and Bouvier, M. (1998) *Biochem. Cell Biol.* **76,** 1–11
62. Lee, S. P., Xie, Z., Varghese, G., Nguyen, T., O'Dowd, B. F., and George, S. R. (2000) *Neuropsychopharmacology* **23,** S32–40
63. Salahpour, A., Angers, S., and Bouvier, M. (2000) *Trends Endocrinol. Metab.* **11,** 163–168
64. Bouvier, M. (2001) *Nat. Rev. Neurosci.* **2,** 274–286
65. Yesilaltay, A., and Jenness, D. D. (2000) *Mol. Biol. Cell* **11,** 2873–2884
66. Willey, R. L., Bonifacino, J. S., Potts, B. J., Martin, M. A., and Klausner, R. D. (1988) *Proc. Natl. Acad. Sci. U. S. A.* **85,** 9580–9584
67. Howard, O. M., Shirakawa, A. K., Turpin, J. A., Maynard, A., Tobin, G. J., Carrington, M., Oppenheim, J. J., and Dean, M. (1999) *J. Biol. Chem.* **274,** 16228–16234
68. Paxton, W. A., Liu, R., Kang, S., Wu, L., Gingeras, T. R., Landau, N. R., Mackay, C. R., and Koup, R. A. (1998) *Virology* **244,** 66–73